

# Lead electrodeposition from very alkaline media

Sheila M. Wong, Luísa M. Abrantes<sup>\*,1</sup>

*CQB, Departamento de Química e Bioquímica, Faculdade de Ciências, Universidade de Lisboa,  
Campo Grande, 1749-016 Lisboa, Portugal*

Received 1 April 2005; received in revised form 20 May 2005; accepted 23 May 2005  
Available online 27 June 2005

## Abstract

The electrodeposition of lead from very alkaline media has been studied by cyclic voltammetry, chronoamperometry under stationary and convective conditions. Experimental parameters like lead concentration and temperature have been varied. From NaOH 6 M the metal deposition takes place at about  $-0.90$  V versus SCE far from the hydrogen evolution reaction (HER) which is seen at  $-1.30$  V, but both processes are favoured by the lead content increase and the NaOH concentration decrease. The analyses of the chronoamperometric responses support the view of a 3D growth and suggest a substantial influence of lead concentration on the type of nucleation. Progressive nucleation is observed for the deposition from solutions with low content in lead but as this concentration increases a tendency towards instantaneous nucleation is revealed. The voltammetry with the rotating platinum disc electrode has confirmed that the lead electrodeposition is a mass transfer controlled process, and also allowed the estimation of diffusion coefficients.

© 2005 Elsevier Ltd. All rights reserved.

**Keywords:** Lead electrodeposition; Alkaline media; Nucleation; Growth

## 1. Introduction

Lead electrodeposition has been subject of interest in several investigations due to its potential application in relevant technologies, such as the production of high purity active material for acid battery [1], for semiconductors [2,3] and the fabrication of electrochromic devices [4–6]. On the other hand, lead long-term toxicity is considered a very relevant environmental problem and thus other works have been dedicated to the study of lead electrochemical deposition either for the direct detection of the metal [7,8] or for its recycling [9–11].

For the research on lead electrodeposition, the most used electrolytes are acid and based on chloride [9,12,13], bromide [14], iodide [14], nitrate [6] and fluoborate [15]. In these solutions lead is mainly present as  $Pb^{2+}$ , but lead(II)–halide complexes can also be formed, as in high concentration of chloride solutions where soluble complexes, e.g.,  $PbCl^+$ ,  $PbCl_3^-$  and

$PbCl_4^{2-}$  are found and chlorine evolution can occur as a competitive reaction [10,14]. In spite of most acid electrolytes being considered toxic and alkaline solutions assumed as more appropriate from an environmental standpoint [11], the literature is poor in reports related to alkaline media. To our knowledge, the most recent study on lead electrodeposition from this medium was performed using copper as substrate in alkaline glycerol media [16]. The authors consider that the reduction of lead occurs entirely through the complex species  $[Pb(OH)_4]^{2-}$  and not  $Pb^{2+}$ , describe the formation of lead deposits presenting potential use in the production of high purity lead, and study the viability of glycerol as additive. Steel 1010 has also been used as cathode material in the production of lead powder and for waste treatment, in particular lead-acid batteries [11,17]. Other investigations, carried out in alkaline media give emphasis to lead electro-winning for metal recovery without any detailed kinetic approach [18–21].

In metal electrodeposition, a convenient method to investigate the nucleation and growth mechanism is by chronoamperometry applying the literature well described models: Harrison et al. developed  $I-t$  theoretical relations

\* Corresponding author. Tel.: +351 217500890; fax: +351 217500088.

E-mail address: [luisa.abrantes@fc.ul.pt](mailto:luisa.abrantes@fc.ul.pt) (L.M. Abrantes).

<sup>1</sup> ISE member.

for two-dimensional (2D) growth by instantaneous and progressive nucleation [22] and three-dimensional (3D) growth is considered in the known Scharifker–Hills (SH) model, which also describes both types of nucleation, assuming diffusion-controlled growth [12]. The SH model has been applied in several electrodeposition studies [23–28], including the case of lead [3,29].

Lead electrodeposition on zinc oxide, from 50 mM Pb(NO<sub>3</sub>)<sub>2</sub> in aqueous KNO<sub>3</sub>, has been reported as a 3D growth with instantaneous nucleation [12]. The same type of assignment for the lead nucleation and growth, on indium–tin oxide from similar electrolyte solutions has recently been reported [5], as well as on germanium from more acidic medium, 5 mM Pb(ClO<sub>4</sub>)<sub>2</sub> + 0.1 M NaClO<sub>4</sub> + 10 mM HClO<sub>4</sub> [3]. Some nucleation studies consider the presence of halides and state that mass transport to growing nuclei seems not to be affected by the formation of soluble lead–halides complexes due to similar diffusion coefficient values, about  $11 \times 10^{-6} \text{ cm}^2 \text{ s}^{-1}$  [14]. Equivalent values for the diffusion coefficient [13,30] are also reported in studies concerning lead electrodeposition from neutral and acid media.

Since the mechanism of lead electrodeposition from very alkaline media has been disregarded to date, it seemed to be interesting to study the formation of the new metallic phase on platinum and on stainless steel. The results obtained by voltammetry and by chronoamperometry from NaOH 6 M solution are here presented and the current transients analysed under the light of the SH model.

## 2. Experimental

Lead electrodeposition was carried out on Pt and stainless steel AISI 316 (SS316) from aqueous solutions of PbO (2.41–48.3 mM Pb(II)) in NaOH (3–6 M). All solutions were prepared using analytical grade reagents and Millipore water (18 MΩ cm). Before each experiment the electrolyte solutions were de-aerated by bubbling high pure N<sub>2</sub> for 15 min.

Electrodeposition was performed in a conventional three-electrode electrochemical cell with a saturated calomel electrode (SCE) as reference and a Pt foil counter electrode. The Pt and the SS316 working electrodes, discs of 0.196 cm<sup>2</sup>, and a Pt rotating disc electrode (RDE) of 0.385 cm<sup>2</sup>, were polished with alumina suspension of 1.0 and 0.3 μm to a mirror bright finishing, before each experiment.

The lead reduction and oxidation processes were investigated by cyclic voltammetry within –1.8 and 1.0 V potential domain, at 50 mV s<sup>-1</sup>; a smaller potential window (–1.2 to –0.7 V) was also explored at several sweep rates (1–300 mV s<sup>-1</sup>). The nucleation and growth mechanism was studied for 24.1 and 48.3 mM Pb(II) in NaOH 6 M aqueous solutions, through the treatment of chronoamperograms obtained with potential pulses from the open circuit potential to different final potentials,  $E_f = -0.875$  to  $-0.905$  V. Stationary experiments were carried out using a Amel Instruments potentiostat (model 2055), with Wenking Voltage Scan

Generator (model VSG 83) and Goerz recorder (Servogor 790) whereas the influence of temperature (<50 °C) and convection (<60 s<sup>-1</sup>) on the reduction processes, studied by linear voltammetry, were performed with a Radiometer Potentiostat (DEA 332 Digital Electrochemical Analyser, IMT 102 Electrochemical Interface), equipped with a Voltmaster 2 program (version X9824-2.01, number 903V201/INT) for data acquisition. A Thermomix thermostat (UB, B. Braun) was used for temperature control and convection provided by an EG&G rotating disk electrode (PARC model 616 RDE).

## 3. Results and discussion

Accordingly with literature, both Pb(OH)<sub>3</sub><sup>-</sup> and Pb(OH)<sub>4</sub><sup>2-</sup> species could be considered under the present conditions (48.3 mM Pb(II) in NaOH 6 M). From the reported information for Pb(OH)<sub>4</sub><sup>2-</sup>/Pb [17,31] the formal potential of lead electrodeposition has been worked out and the agreement with the observed value provides support for the assumption of Pb(OH)<sub>4</sub><sup>2-</sup> as the most abundant lead species.

The cyclic voltammograms obtained at Pt, between –1.8 and 1.0 V, is shown in Fig. 1. Starting from the open circuit potential (ocp), –0.15 V, towards the negative direction, at about  $E = -0.90$  V it can be observed a peak (R1) that

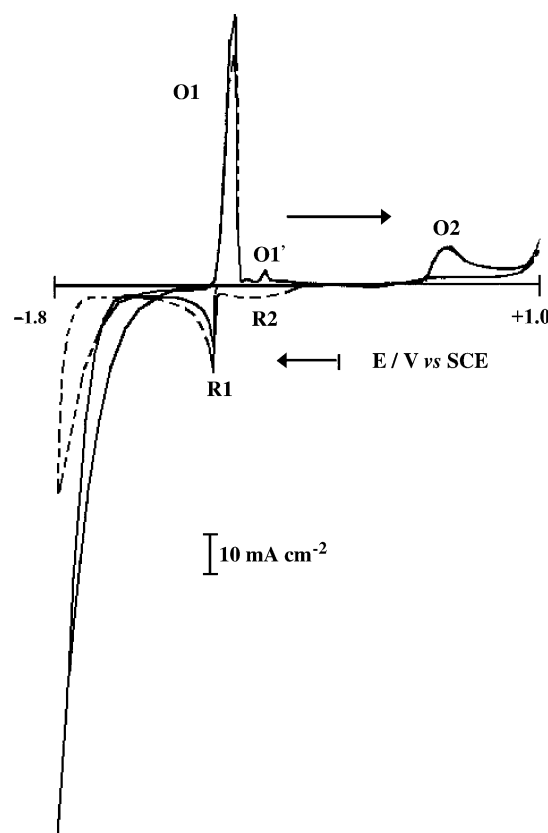


Fig. 1. Cyclic voltammetric responses of Pt in 48.3 mM Pb(II) + NaOH 6 M: (—) first and (---) second cycle, starting from the ocp (–0.15 V) and sweeping the potential in the negative direction;  $\nu = 50 \text{ mV s}^{-1}$ .

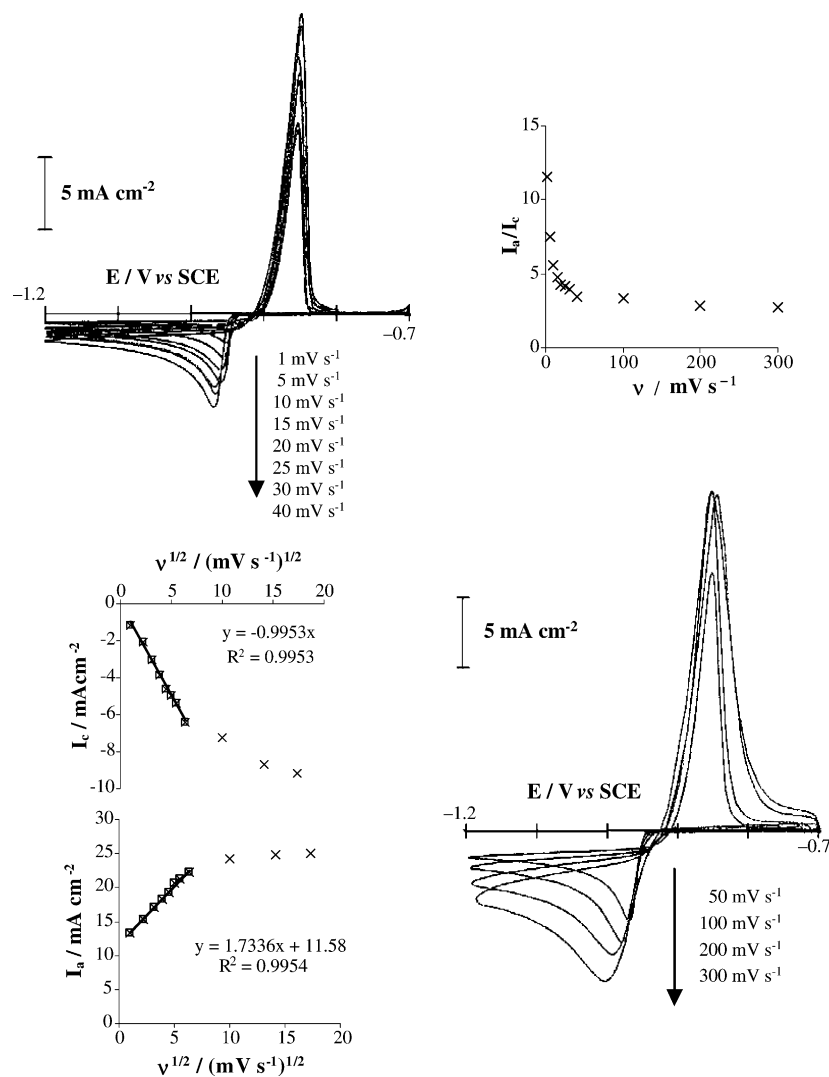
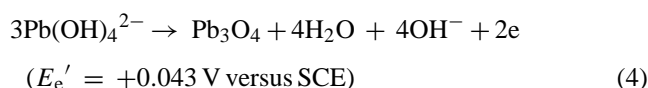
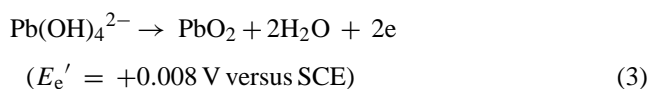
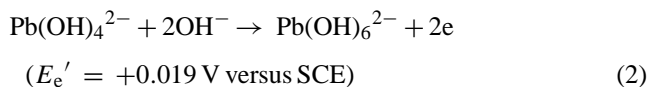


Fig. 2. Cyclic voltammograms for SS316 in 24.1 mM Pb(II) + NaOH 6 M, at different potential sweep rates (from 1 to 300  $\text{mV s}^{-1}$ ) and respective data treatment.

corresponds to the lead deposition, and the hydrogen evolution reaction (HER) at  $-1.40$  V. In the reverse positive direction the lead dissolution is denoted by the stripping peak O1 occurring at  $-0.78$  V, followed by a relatively small oxidation peak O1' at  $-0.59$  V. By the analysis of the equilibrium reactions involving this lead(II)–hydroxide complex reported in literature [31], it is possible to assign the redox couple R1/O1 to reaction (1) which equilibrium potential  $E'_e = -0.910$  V versus SCE was estimated considering the experimental conditions used in this work:



At more positive potentials,  $0.46$  V, the oxidation peak O2 shall denote the formation of lead oxides and/or lead(IV) soluble species according to the reactions (2)–(4):



Reversing again the potential sweep, the current crossover at about  $0.40$  V supports the occurrence of the lead oxides deposition (Eqs. (3) and (4)). The subsequent cycle shows a broad peak R2 just before the lead deposition area, and the Pt surface modification is clearly responsible for the higher overpotential for the HER. Starting from ocp and sweeping the potential in the positive direction the behaviour is identical except for the peak R2 which is observed on the 1st of cycle, suggesting that it is the counterpart of the oxidation denoted by the peak O2.

The cyclic voltammograms obtained for SS316 in aqueous solution containing 24.1 mM Pb(II) in 6 M NaOH are

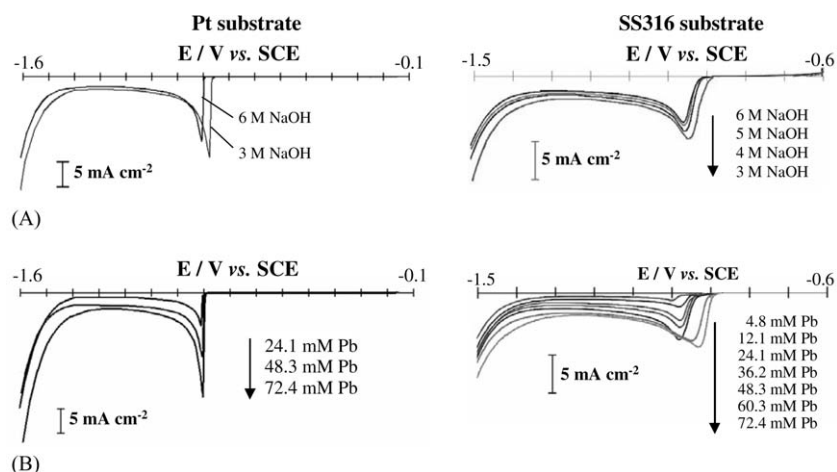


Fig. 3. Linear voltammograms obtained for Pt and SS316 electrodes in (A) 48.3 mM Pb(II) + NaOH 3, 4, 5, 6 M, and (B) 4.83, 12.1, 24.1, 36.2, 48.3, 60.3 and 72.4 mM Pb(II) in 6 M NaOH;  $\nu = 20 \text{ mV s}^{-1}$ .

illustrated in Fig. 2. On this substrate a slightly higher overpotential is required for the lead electrodeposition. The data (inlets of Fig. 2) points to a quasi-reversible system [32–34] since the anodic to cathodic current peaks ratio,  $I_a/I_c$ , obtained at several sweep rates,  $\nu$ , is higher than unity and decreases with the increase in  $\nu$ ,  $I_a$  and  $I_c$  values are directly proportional to the  $\nu^{1/2}$  and  $\Delta E \cong 80 \text{ mV}$ , below  $40 \text{ mV s}^{-1}$ ; the peak separation increases with  $\nu > 40 \text{ mV s}^{-1}$ . Similar characteristics were observed in the voltammograms recorded with Pt electrode.

The influence of lead and NaOH concentration, on the lead deposition process on Pt and on SS316 is shown in Fig. 3. These results suggest that as the ratio  $[\text{Pb}]/[\text{NaOH}]$  increases the metal deposition involves other present species, very

likely  $\text{Pb}(\text{OH})_3^-$ . It can be seen that the electrodeposition occurs at less negative potential values as NaOH concentration becomes smaller and lead content increases, being the effect more noticeable when SS316 is used; on these substrate the HER is also favoured.

Fig. 4 depicts the linear voltammograms recorded at different temperatures under convective conditions. Although a quantitative analysis of the data from RDE voltammetry will be presented later, it is worthwhile to point some features of the current responses. On Pt (Fig. 4A–C) the lead deposition potential is not relevantly altered by the temperature modification or by the electrode rotation up to  $5 \text{ s}^{-1}$  angular velocity,  $\omega$ , but the potential at which the HER occurs is significantly shifted towards less negative values; the same behaviour is

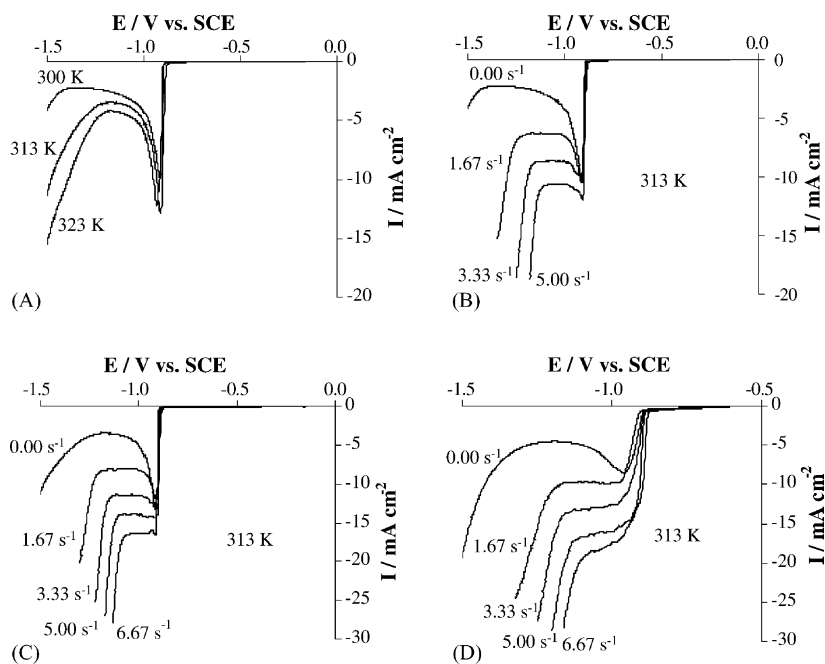


Fig. 4. Linear voltammograms recorded in 48.3 mM Pb(II) + NaOH 6 M at (A)  $T = 300, 313$  and  $323 \text{ K}$ , (B)  $\omega = 0, 1.67, 3.33$  and  $5.00 \text{ s}^{-1}$ , (C)  $T = 313 \text{ K}$ ,  $\omega = 0, 1.67, 3.33, 5.00$  and  $6.67 \text{ s}^{-1}$  on Pt and on SS316 (D) under the same conditions as (C);  $\nu = 20 \text{ mV s}^{-1}$ .

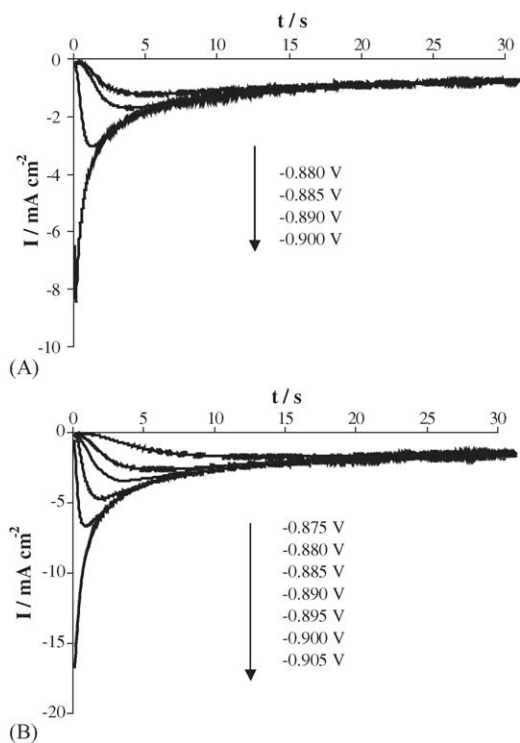


Fig. 5. Current transients for potentiostatic Pb deposition on Pt from (A) 24.1 and (B) 48.3 mM Pb(II) in NaOH 6 M, with  $E = -0.875, -0.880, -0.885, -0.890, -0.895, -0.900$  and  $-0.905$  V.

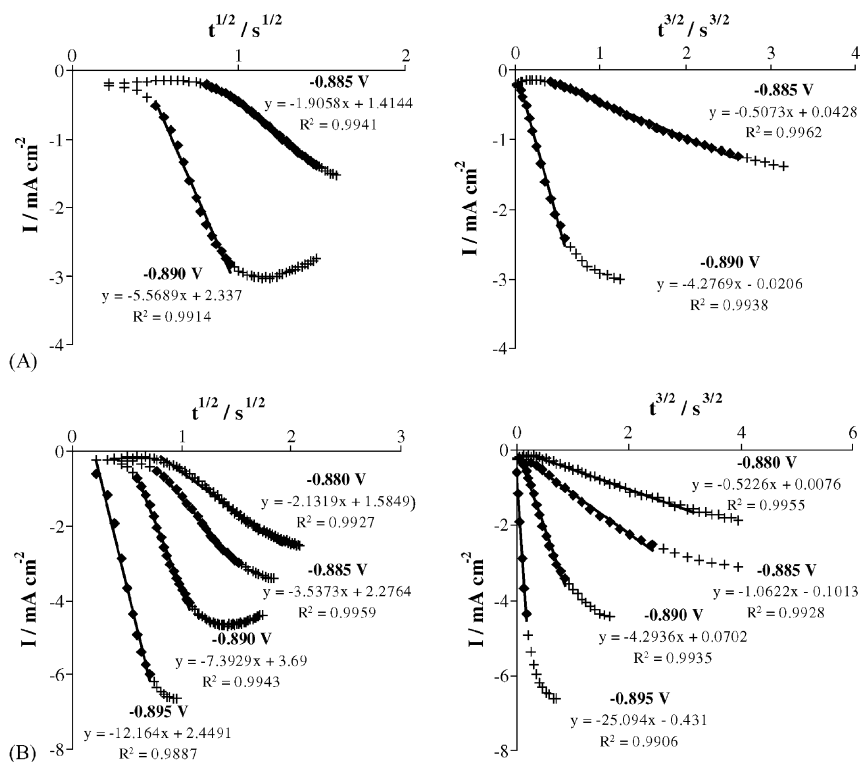


Fig. 6. Plots of  $I$  vs.  $t^{3/2}$  and  $I$  vs.  $t^{1/2}$  for Pb deposition onto Pt, from (A) 24.1 and (B) 48.3 mM Pb(II) in NaOH 6 M (data from Fig. 5).

observed for stainless steel (Fig. 4D). As expected, the use of forced convection increases the rate of the metal deposition process but high  $\omega$  also contributes to close by the competitive HER.

A detailed chronoamperometric study was carried out to investigate the early stages of lead phase formation on Pt, i.e., the electrocrystallization and kinetic features. The widely known theory treated by Scharifker and Hills [12] has been used. For different applied potentials, from  $-0.875$  to  $-0.905$  V, the collected current transients are presented in Fig. 5.

For pulses higher than  $-0.880$ , curves show a typical response of a three-dimensional (3D) multiple nucleation with diffusion controlled growth [12], with a steep current increase to a maximum ( $I_m$ ), in a period  $t_m$ . Accordingly, the rising current is either due to the growth of the new phase and/or to an increase of the number nuclei; during this stage of deposited lead growth, the nuclei develop diffusion zones which may overlap changing the hemispherical into a linear mass-transfer and resulting in an effectively planar surface, the current then falls to the limiting diffusion current for the deposition process.

The early stages of the deposition (rising portion of the transient) was analyzed considering no overlapping of growing nuclei, i.e., only isolated growing nuclei present on the surface. The plots of  $I$  versus  $t^{1/2}$  and  $I$  versus  $t^{3/2}$  for instantaneous and progressive nucleation, respectively, Fig. 6, indicate the occurrence of instantaneous nucleation in the case of the higher lead concentration (a good linearity

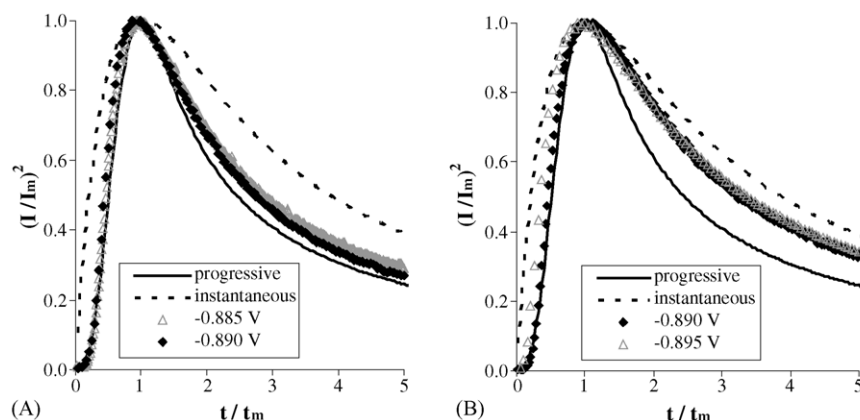


Fig. 7. Theoretical and experimental non-dimensional plots  $(I/I_m)^2$  vs.  $t/t_m$  for Pb deposition onto Pt, from (A) 24.1 and (B) 48.3 mM Pb(II) in NaOH 6 M (data from Fig. 5).

is obtained for  $I$  versus  $t^{1/2}$ ); for the case of 24.1 mM Pb(II), the results appear to point to a progressive process.

A more detailed analysis, based on normalized current data, as function of  $I_m$  and  $t_m$ , for instantaneous and progressive growth, concerning the 3D multiple nucleation with diffusion controlled growth [12] was performed as illustrated by Fig. 7. Indeed, in the case of metal deposition on Pt from 24.1 mM Pb(II) solution (Fig. 7A), the experimental data is clearly close to the theoretical curve representing a progressive nucleation whereas in what concerns the 48.3 mM Pb(II) solution (Fig. 7B), the data lies between the theoretical curves of each type of nucleation, pointing to an instantaneous nucleation when high lead concentrations are used. It is worth to mention that the fitting uses almost the whole current transient, in particular at the smallest lead concentration; the studied system shall present 3D multiple nucleation with diffusion controlled growth and thus the type of nucleation appears dependent on the solution composition showing tendency to instantaneous at high values of lead concentration.

Further evidence for the nucleation type has been obtained from  $I_m^2 t_m$  expression [5,12] assuming that its value is independent of the nucleation and growth rate, i.e., at a given bulk concentration of electrodepositing species,  $I_m^2 t_m$  should not vary with the overpotential for sufficiently high potentials pulses. The theoretical value was determined using  $D$  estimated from the Cottrell equation (Fig. 8), applied to the decaying portion of the current transient recorded with the highest overpotential, and compared with the experimental one shown in Fig. 5. As it can be seen in Table 1, the  $I_m^2 t_m$  values confirm the progressive nucleation for the deposition

Table 1  
 $I_m^2 t_m$  experimental and theoretical values for instantaneous and progressive nucleation

[Pb] (mM)	$D$ ( $\text{cm}^2 \text{s}^{-1}$ )	$I_m^2 t_m$		
		Experimental	Instantaneous	Progressive
24.1	$2.44 \times 10^{-6}$	$1.2 \times 10^{-5}$	$8.62 \times 10^{-6}$	$1.38 \times 10^{-5}$
48.3	$2.53 \times 10^{-6}$	$4.2 \times 10^{-5}$	$3.58 \times 10^{-5}$	$5.70 \times 10^{-5}$

from the most diluted used solution and closer to an instantaneous process when 48.3 mM Pb(II) is employed.

For the progressive nucleation case (lead deposition from 24.1 mM Pb(II)), the analysis of the transients also allows the evaluation of the combined nucleation parameters  $AN_0$  ( $A$  is the nucleation rate constant and  $N_0$  the density of active sites) providing  $6.1 \times 10^4$  and  $6.0 \times 10^5 \text{ s}^{-1} \text{ cm}^{-2}$  for electrodeposition at  $-0.885$  and  $-0.890$  V, respectively.

RDE voltammetry was used to analyse the influence of lead concentration on diffusion limiting step of the electrodeposition. The technique also allowed the diffusion coefficient estimation for a wide range of lead concentrations. Fig. 9 shows a series of voltammograms in the hydrodynamic mode for NaOH 6 M solutions containing different lead concentrations. All the curves present a well-defined limiting current plateau,  $I_L$ , over a large potential range especially in the case of the smaller lead concentration used. The potential window at which the current is limited by diffusion decreased as the lead content in solution increased, due to the promotion of HER at less negative potential values. This competitive reaction occurs beyond 1.30 V without electrode rotation, but with  $\omega = 34.54 \text{ s}^{-1}$  for the series of curves obtained for Pt-RDE in 48.3 mM Pb(II) and NaOH 6 M the HER starts at  $-1.03$  V. This behaviour suggests that

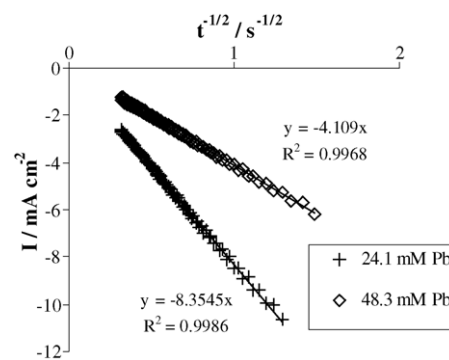


Fig. 8. Cottrell plots for the chronoamperograms of Fig. 5 ( $-0.900$  and  $-0.905$  V for 24.1 and 48.3 mM Pb(II), respectively).

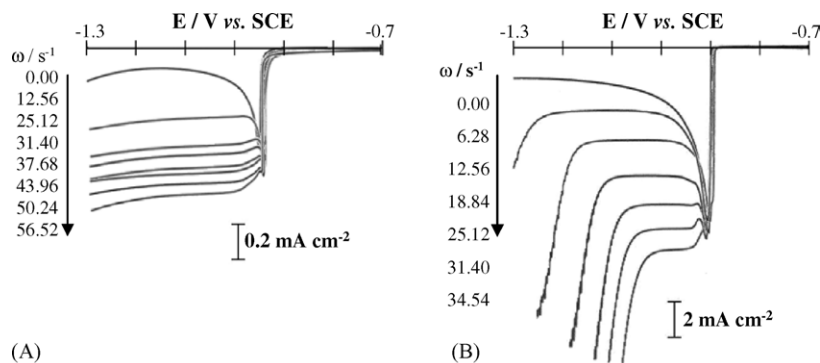


Fig. 9. Linear voltammograms obtained for Pt-RDE in (A) 24.1 and (B) 48.3 mM Pb(II) in NaOH 6M, at different  $\omega$ ;  $\nu = 10 \text{ mV s}^{-1}$ .

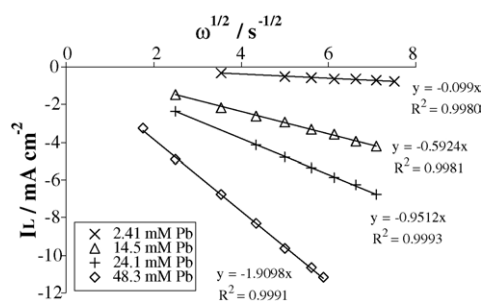


Fig. 10. Levich plots for linear voltammograms obtained with electrode rotation ( $\omega$ ) in NaOH 6M solutions with 2.41, 14.5, 24.1 and 48.3 mM Pb(II).

the accepted mechanism for the hydrogen evolution reaction on Pb in acid media (proton discharge-rate determining followed by electroodic desorption) is not prevalent in alkaline media. However, on a particularly active lead deposit, a rate determining diffusion of molecular hydrogen away from the electrode surface might explain the apparent electrocatalytic activity for water reduction (Fig. 9B).

The limiting current density dependence on the Pt-RDE rotation rate, characteristic of a mass-transfer controlled process, was verified applying the Levich equation [35–37]. The  $I_L$  (measured at a mid point of the plateaus) plotted against  $\omega^{1/2}$  is presented in Fig. 10; the obtained linear relation confirms the mass transfer control and allows the  $D$  estimation for each concentration used (Table 2) which are in good agreement with the values evaluated from chronoamperometric data (Table 1) and suggest a weak influence of the lead concentration, since a very small increase is observed with the lowering of lead concentration. These values are lower than the known [11] for lead in a NaOH

2 M solution ( $4.0 \times 10^{-6} \text{ cm}^2 \text{ s}^{-1}$ ) likely due to the relatively smaller pH value used. From neutral and acid medium it has been reported [13]  $D \approx 10 \times 10^{-6} \text{ cm}^2 \text{ s}^{-1}$  in the presence of 10–20 mM Pb(II) and pointed out a tendency to smaller  $D$  values as lead concentration is increased.

#### 4. Conclusions

The electrodeposition of lead from very alkaline media takes place at about  $-0.90 \text{ V}$  versus SCE being the HER less competitive since it only occurs at  $-1.30 \text{ V}$ . The deposition process and the HER are favoured by the increase of lead content and the decrease of NaOH concentration. Once the metal is deposited, scanning the potential anodically, lead oxides formation, most probably  $\text{PbO}_2$  and  $\text{Pb}_3\text{O}_4$ , and  $\text{Pb}(\text{OH})_6^{2-}$  is observed.

Besides the expected effect upon the quantity of deposited metal (increases) and on the potential of HER (decreases), temperatures high as  $50^\circ \text{C}$  and forced convection up to  $\omega = 60 \text{ s}^{-1}$  do not influence the potential at which deposition starts.

The analysis of the chronoamperometric responses reveals a 3D growth and a relevant influence of lead concentration on the type of nucleation: in the presence of 24.1 mM Pb(II) the results point to a progressive nucleation and as the lead concentration increases a tendency towards instantaneous nucleation shall be expected.

Under the studied conditions, the lead electrodeposition is a mass transfer controlled process as revealed by RDE voltammetry. The data also allows to estimate the diffusion coefficients which present a small increase from  $D = 2.65 \times 10^{-6} \text{ cm}^2 \text{ s}^{-1}$  to  $D = 2.80 \times 10^{-6} \text{ cm}^2 \text{ s}^{-1}$  as the lead concentration is decremented from 48.3 down to 2.41 mM.

Table 2  
Limiting current densities and diffusion coefficients obtained from data shown in Fig. 9

[Pb] (mM)	$I_L$ ( $\omega = 25.12 \text{ s}^{-1}$ ) ( $\text{mA cm}^{-2}$ )	$D$ ( $\times 10^{-6} \text{ cm}^2 \text{ s}^{-1}$ )
2.41	-0.49	2.79
14.5	-2.93	2.79
24.1	-4.81	2.63
48.3	-9.62	2.65

#### References

- [1] D. Pavlov, J. Power Sources 42 (1993) 345.
- [2] B. Rashkova, B. Guel, R.T. Potzschke, G. Staiikov, W.J. Lorenz, Electrochim. Acta 43 (1998) 3021.

- [3] C. Ehlers, U. Konig, G. Staikov, J.W. Schultze, *Electrochim. Acta* 47 (2001) 379.
- [4] L.H. Mascaró, E.K. Kaibara, L.O. Bulhões, *J. Electrochem. Soc.* 144 (10) (1997) L273.
- [5] L.O.S. Bulhões, L.H. Mascaró, *J. Solid State Electrochem.* 8 (2004) 238.
- [6] C.O. Avellaneda, M.A. Napolitano, E.K. Kaibara, L.O.S. Bulhões, *Electrochim. Acta* 50 (2005) 1317.
- [7] J. Saterlay, C. Agra-Gutiérrez, M.P. Taylor, F. Marken, R.G. Compton, *Electroanalysis* 11 (1999) 1083.
- [8] C. Prado, S.J. Wilkins, P. Grundler, F. Marken, R.G. Compton, *Electroanalysis* 15 (12) (2003) 1011.
- [9] L. Doulikas, K. Novy, S. Stucki, Ch. Comninellis, *Electrochim. Acta* 46 (2000) 349.
- [10] E. Exposito, J. Iniesta, J. González-García, V. Montiel, A. Aldaz, *J. Power Sources* 92 (2001) 260.
- [11] I.A. Carlos, J.L.P. Siqueira, G.A. Finazzi, M.R.H. de Almeida, *J. Power Sources* 117 (2003) 179.
- [12] B. Scharifker, G. Hills, *Electrochim. Acta* 28 (1983) 879.
- [13] J. Mostany, J. Mozota, B.R. Scharifker, *J. Electroanal. Chem.* 177 (1984) 25.
- [14] J. Mostany, J. Parra, B.R. Scharifker, *J. Appl. Electrochem.* 16 (1986) 333.
- [15] E. Expósito, J. González-García, P. Bonete, V. Montiel, A. Aldaz, *J. Power Sources* 87 (2000) 137.
- [16] I.A. Carlos, T.T. Matsuo, J.L.P. Siqueira, M.R.H. de Almeida, *J. Power Sources* 132 (2004) 261.
- [17] I.A. Carlos, A. Malaquias, M.M. Oizumi, T.T. Matsuo, *J. Power Sources* 92 (2001) 56.
- [18] C. Weiping, T. Yizhunang, B. Kerun, Z. Yue, *Trans. Nonferr. Met. Soc. Chin.* 6 (1996) 47.
- [19] C. Weiping, C. Fancai, P. Yanbing, L. Qizhong, B. Kejun, Z. Yue, *Trans. Nonferr. Met. Soc. Chin.* 7 (1997) 154.
- [20] A.G. Morachevskii, A.I. Demidov, Z.I. Vaisgant, M.S. Kogan, *Russ. J. Appl. Chem.* 70 (1997) 1.
- [21] L.C. Ferracin, A.E. Chácon-Sanhueza, R.A. Davoglio, L.O. Rocha, D.J. Caffeu, A.R. Fontanetti, R.C. Rocha-Filho, S.R. Biaggio, N. Bocchi, *Hydrometallurgy* 65 (2002) 137.
- [22] J.A. Harrison, H.R. Thirsk, A.J. Bard (Eds.), *Electroanalytical Chemistry*, vol. 5, Marcel Dekker, New York, 1971, p. 67.
- [23] H. Cesiulus, M. Ziomek-Moroz, *J. Appl. Electrochem.* 30 (2000) 1261.
- [24] G. Oskam, P.C. Searson, *J. Electrochem. Soc.* 147 (2000) 2199.
- [25] D. Grujicic, B. Pesic, *Electrochim. Acta* 47 (2002) 2901.
- [26] M.E. Quayum, S. Ye, K. Uosaki, *J. Electroanal. Chem.* 520 (2002) 126.
- [27] S.B. Sadale, P.S. Patil, *Solid State Ionics* 167 (2004) 273.
- [28] A.E. Alvarez, D.R. Salinas, *J. Electroanal. Chem.* 566 (2004) 393.
- [29] J.C. Ziegler, R.I. Wielgosz, D.M. Kolb, *Electrochim. Acta* 45 (1999) 827.
- [30] F. Palmisano, E. Desimoni, L. Sabbatini, G. Torsi, *J. Appl. Electrochem.* 9 (1979) 571.
- [31] R.A. Lidin, V.A. Molochko, L.L. Andreeva, *Reactivity of Inorganic Substances*, Begell House Inc., New York, 1996.
- [32] P.-Y. Chen, I.-W. Sun, *Electrochim. Acta* 45 (2000) 3163.
- [33] Y. Katayama, S. Dan, T. Miura, T. Kishi, *J. Electrochem. Soc.* 148 (2001) C102.
- [34] M. Morimitsu, Y. Nakahara, Y. Iwaki, M. Matsunaga, *J. Min. Metall.* 39B (1–2) (2003) 59.
- [35] V.G. Levich, *Physicochemical Hydrodynamics*, Prentice-Hall, Englewood Cliffs, NJ, 1962.
- [36] E. Elsherief, *Electrochim. Acta* 48 (18) (2003) 2667.
- [37] J. Jiang, A. Kucernak, *Electrochim. Acta* 47 (12) (2002) 1967.